

## Seismic protection of vulnerable equipment with semi-active control by employing robust and clipped-optimal algorithms

H. Salehi<sup>1</sup>, T. Taghikhany<sup>2,\*</sup>, A. Yeganeh Fallah<sup>3</sup>

Received: April 2013, Revised: October 2013, Accepted: December 2013

### Abstract

Critical non-structural equipments, including life-saving equipment in hospitals, circuit breakers, computers, high technology instrumentations, etc., are vulnerable to strong earthquakes, and the failure of these equipments may result in a heavy economic loss. To guarantee function of vulnerable equipment during earthquakes, peak acceleration and peak base displacement response of the system should be limited to allowable levels. Traditional and passive control strategies cannot afford these contradictory targets at the same time for broad range of ground motions. In recent years, semi-active control systems have been introduced as an adaptable and reliable alternative to control response under both limitations with low power supply.

In this paper, efficacy of the smart semi-active controlled floor isolation system, which consists of a rolling pendulum system and a semi-active controlled magnetorheological (MR)-damper to control seismic response of equipment, has been investigated by using clipped- $H_2$ /LQG and clipped- $H_\infty$  algorithms. The effectiveness of these algorithms was examined for the equipment stand on a raised floor due to floor motions in a seven storey building. The results demonstrate that semi-active control effectively decreases response acceleration and velocity of equipment in comparison to passive strategy and holds its relative displacement to floor in least value. Furthermore, it was shown semi-active control strategy with clipped- $H_\infty$  algorithm compared to clipped- $H_2$ /LQG algorithm and passive strategy (isolation system) has a better performance in protecting equipment.

**Keywords:** Semi-active control, MR-damper,  $H_\infty$  algorithm,  $H_2$ /LQG algorithm, Equipment.

### 1. Introduction

While security improvement of bridges, power plants, and dams against earthquakes have attracted special attention during recent years, fewer efforts are launched for the improvement of the operation of critical equipment and its process during and after an earthquake. According to historical records, economical loss due to earthquakes as nonstructural damages can be more than structural ones. In the Northridge Earthquake, for example, many facilities and devices were damaged and malfunctioned [1].

Because the performance of highly sensitive equipment in hospitals, communication centers, and computer facilities can be easily disrupted by moderate acceleration levels and even permanently damaged by higher excitations, efforts have turned toward the use of isolation for protection of a building's contents [2].

Application of passive control strategy in the form of isolation system is one of the common methods in protection of equipment.

Lambrou and Constantinou, underwent some comprehensive shake table tests on Friction Pendulum Isolation Systems (FPS) of a raised floor under seismic loads. They demonstrated the efficacy of an isolated raised floor to reduce input acceleration to equipment over flooring [3-4]. However, excessive displacement for the isolator during high-amplitude and long period ground motions, such as near-fault excitations, could damage the isolation system and the equipment. Thus, in order to secure function of vulnerable equipment in earthquakes, their response acceleration and base displacement should be simultaneously limited to allowable levels. These contradictory performance objects cannot be achieved without smart and adaptable protecting system.

In recent years a lot of research has been conducted towards evaluation of active control strategy for earthquake protection of sensitive equipment. In 2000, a comprehensive numerical study was carried out by Yang and Agrawal on applicability of various protective systems for both micro vibration control and seismic response control of sensitive equipment [5]. Xu et al. studied a hybrid platform consisting of passive mounts and actively

\* Corresponding author: ttaghikhany@aut.ac.ir

1 Master of Science, Department of Civil and Environmental Engineering, Amirkabir University of Technology, Tehran, Iran

2 Assistant Professor, Department of Civil and Environmental Engineering, Amirkabir University of Technology, Tehran, Iran

3 Ph.D. Candidate, Department of Civil and Environmental Engineering, Amirkabir University of Technology, Tehran, Iran

controlled hydraulic actuators to protect high tech equipments against traffic induced micro vibration without considering earthquake. Xu and Li explored the possibility of using a double-layer passive isolation platform and hybrid platform with magnetostrictive actuators to ensure the functionality of high-tech equipment when an earthquake occurs [6-7]. They established Linear Quadratic Gaussian (LQG) algorithms to control magnetostrictive actuators. In active control strategy, the stiffness and damping of plants are being varied online by actuator action to minimize dynamic responses. This enables equipment to continue servicing after an earthquake. However, there are serious questions about their reliability and power supply to protect sensitive equipment during earthquake.

Meanwhile, semi-active control strategy holds adaptability of active system in effective reduction of response during extensive arrangement of the dynamic loading conditions without need of the big energy resource; it insures stability of the system at the time of loading like passive strategy (Christenson, 2001). The semi-active device is in different forms, such as variable friction dampers (Yang and Agrawal, 2002; Lu et al. 2004; Chen and Chen, 2004), or variable fluid devices, like MR or ER dampers (Sahasrabudhe and Nagarajaiah, 2005; Symans and Constantinou, 1997; Dyke et al. 1998) [8-13].

Currently, magnetorheological (MR) dampers are being widely studied for their potential use as semi-active control devices. The isolator, such as LRB, RB and FPS, provide the vertical support with suitable lateral stiffness and hysteresis. To enhance the control effect or to reduce the stroke of the isolation system, the energy dissipation devices (such as hydraulic dampers) are added. For the same reason, the semi-active controlled MR damper is good to use in the hybrid controlled base isolation system. In 2007, Shook et al. had an analytical and experimental study on hybrid isolation system that is comprised of a bidirectional roller-pendulum system and MR dampers to reduce the potential for damage to structures and sensitive equipment. They examined three contrasting control techniques include neural network, LQR/clipped-optimal and fuzzy logic control [14]. They revealed all considered control methods effectively alleviated the seismic response of equipment but the LQR/clipped-optimal controller with variable gains is superior to the other controllers. Lin and Loh had shaking table experimental tests on a three-storey steel structure with the floor isolation system on the 2nd floor. They investigated two contrasting control methods including LQR with continuous-optimal control and Fuzzy Logic control as potential algorithms and comparisons were made from their results. They showed the semi-active controlled floor isolation system not only can dramatically reduce the floor acceleration responses under various kinds of excitations, but also mitigate the global structural responses [15-16]. Fan et al investigated performance of passive and semi-active control in the equipment isolation system for earthquake protection by conducting shaking table tests on a full-scale three-storey structures. Three control algorithms including the decentralized sliding mode control, LQR-H2 control, and the passive-on and

passive-off control were examined under El Centro, Kobe and Chi-Chi earthquake. Their results illustrated the effectiveness of decentralized sliding mode control, however LQR control performance is poor if both building responses and equipment responses are considered as feedback signals [17].

As shown above, the research on application of semi active strategy in seismic protection of equipment mainly discuss efficiency of various algorithms. Among different introduced algorithms, the robust optimal ones like  $H_\infty$  and  $H_2$ /LQG provide reliable control in a minimum level of expense to protect equipment against earthquake vibration. To date much research has been performed on application of  $H_\infty$  and  $H_2$ /LQG control algorithms and their stability in civil engineering structures. Clipped-optimal control of smart base isolated structures using  $H_2$ /LQG methods with variable damping devices has been studied extensively. Spencer and Ramallo demonstrated the effectiveness of  $H_2$ /LQG in smart base isolation systems [18-21]. Nagarajaiah et al. studied this algorithm for smart base isolated benchmark building with variable friction devices. Clipped-optimal control involves setting the level of semi-active damping force to either maximum or minimum based on the desired active force generated by the  $H_2$ /LQG controller [22]. Robust control methods using  $H_\infty$  have also been studied. Yoshida et al. investigated efficiency of  $H_\infty$  control in vibration isolation for MDOF systems and Jabbari et al. [23] investigated  $H_\infty$  control for seismic excited buildings. Yang and Lin analyzed the  $H_\infty$  control algorithm and its stability for the engineering structures and controlled strategies based on this algorithm to be used in civil engineering structures [24]. Relatively few studies that apply  $H_\infty$  to semi-active control using variable damping semi-active devices have been reported. Narasimhan and Nagarajaiah developed a control algorithm based on  $H_\infty$ . This control algorithm was shown to be effective in reducing the response of base isolated buildings in a set of near-fault earthquakes. It is worth mentioning that efficiency of these algorithms should be investigated when peak acceleration and base displacement have to be limited simultaneously. Because MR dampers have highly nonlinear characteristics, linear optimal control design strategies like  $H_\infty$  and  $H_2$ /LQG are not applicable individually [25].

In this paper, a smart isolation system which consists of a semi-active MR damper and rolling pendulum system is presented. This system can provide the suitable restoring force and vertical support with almost no friction (rolling friction is about 1/1000 of slide friction). The system is investigated in order to protect the equipment stand on a raised floor by means of smart semi-active strategy employing  $H_\infty$  and  $H_2$ /LQG control algorithms. However, application of these algorithms with an MR damper should be combined with a clipped-optimal algorithm to reduce peak acceleration of the equipment, while maintaining base drifts within an acceptable limit. Herein  $H_\infty$ -clipped optimal and  $H_2$ /LQG -clipped optimal are introduced to demonstrate the efficacy of these algorithms in semi-active control of equipment responses due to floor motions in a seven storey building. The effectiveness of the proposed

smart semi-active system is demonstrated through comparison with a passive isolation platform.

## 2. $H_\infty$ Control Problem

The  $H_\infty$  algorithm is a binary control method in which control force and external excitations in simultaneous aspect put the infinity norm of the conversion function between the input of the actuator and a cluster of regulated outputs. This algorithm, due to its specific attributes, is being used in most of the structure control systems for reducing response of the structure.

For the statement of  $H_\infty$  problem, the control structure of a fixed time linear system  $G$ , under input disturbance  $w$  and control force  $u$  can be stated as follows (Nagarajaiah and Narasimhan, [26]):

$$\begin{bmatrix} z \\ y \end{bmatrix} = G(s) \begin{bmatrix} w \\ u \end{bmatrix} = \begin{bmatrix} G_{11}(s) & G_{12}(s) \\ G_{21}(s) & G_{22}(s) \end{bmatrix} \begin{bmatrix} w \\ u \end{bmatrix} \quad (1)$$

In this equation,  $y$  is a measured variable. All the external inputs such as the source signal, disturbance of a system, and the noise of sensors are defined by variable  $w$ .  $z$  is a performance variable and is composed by tracking fault and inputs of actuators. In this situation, control law is as follows:

$$u = k(s)y \quad (2)$$

The  $H_\infty$  control problem is about finding a controller  $K(s)$ , which can stabilize systems such that the effect of the  $w$  disturbance on the  $z$  performance variable is minimized. Herein  $T(s)$  function represents the closed-loop system transfer function from input variable  $w$  to performance variable  $z$ .

$$T(s) = G_{11} + G_{12}k(I - G_{22}k)^{-1}G_{21} \quad (3)$$

Finally, the  $H_\infty$  control problem is about finding controller quality of  $K$ , assuming the given  $\gamma$  and  $T(s)$  transfer function, it may meet the following equation:

$$\|T(s)\|_\infty < \gamma \quad (4)$$

In which,  $\gamma$  is the positive numerical parameter that is selected by the designer for assuring that output rate should be limited under determinate  $H_\infty$  and predetermined quantity compared to the input rate. For the design of the primary  $H_\infty$  controller, we consider the partitioned LTI (Linear Time Invariant) plant  $P$  as follows (Matlab, [27]).

$$P = \begin{bmatrix} A & B_1 & B_2 \\ C_1 & D_{11} & D_{12} \\ C_2 & D_{21} & D_{22} \end{bmatrix} \quad (5)$$

For an  $n$  degree of freedom system,  $A$ ,  $B$ ,  $C$  and  $D$  are the  $2n \times 2n$  system matrix,  $2n \times r$  input matrix,  $2n \times q$  controller location matrix, and  $2n \times p$  feed through matrix respectively.  $q$ ,  $r$  and  $p$  are the number of actuators,

excitation sources, and sensors. In this case, the generalized equations of motion are cast in the following form:

$$\dot{x} = Ax + B_1w + B_2u \quad (6)$$

$$z = C_1x + D_{11}w + D_{12}u \quad (7)$$

$$y = C_2x + D_{21}w + D_{22}u \quad (8)$$

The controller  $K$ , stabilizes the plant  $P$  and has the same number of states as  $P$ . In above equations,  $z$  are the regulated outputs,  $y$  are the measurements,  $x$  are the states, inputs to  $B_1$  are the disturbances, inputs to  $B_2$  are the control inputs, output of  $C_1$  are the errors to be kept small, and output of  $C_2$  are the output measurements provided to the controller.

It is worth mentioning that in order to regulate responses like displacements, velocities and accelerations, the following must be considered: the coefficients  $C_1$ ,  $D_{11}$  and  $D_{12}$  that determine the performance in terms of states  $x$ , control effort  $u$ , and the noise content in the system considering the mathematical model for analysis.

$$C_1 = \begin{bmatrix} 1 & 0 & 0 & 0 \\ 0 & 0 & 1 & 0 \\ E(1,1) & E(1,2) & F(1,1) & F(1,2) \\ 0 & 0 & 0 & 0 \end{bmatrix} D_{11} = \begin{bmatrix} 0 \\ 0 \\ 1 \\ 0 \end{bmatrix} D_{12} = \begin{bmatrix} 0 \\ 0 \\ B_2(3) \\ 1 \end{bmatrix} \quad (9)$$

where, matrices  $E = (-M^{-1}.K)$  and matrices  $F = (-M^{-1}.C)$  and  $E(1,1)$  for instance indicates the first entries (is located in first row and first column) of matrices  $E$ , and  $B_2(3)$  refers to the third entries of vector  $B_2$ .

The solution for the controller for the generalized regulator problem is given by ([28]):

$$f_{opt} = u = -F_\infty \hat{x} \quad (10)$$

And the state estimator is given by:

$$\dot{\hat{x}} = A\hat{x} + B_1(\gamma^{-2}B_1^T X_\infty \hat{x}) + B_2u + Z_\infty L_\infty (C_2 \hat{x} - y) \quad (11)$$

where:

$$F_\infty = -B_2^T X_\infty \quad (12)$$

$$L_\infty = -Y_\infty C_2^T \quad (13)$$

$$Z_\infty = (I - \gamma^{-2}Y_\infty X_\infty)^{-1} \quad (14)$$

There exists a stabilizing controller if and only if there are available positive semi-definite solutions to the two Riccati equations for  $X_\infty$  and  $Y_\infty$  and the condition:

$$\rho(X_\infty Y_\infty) = \gamma^2 \quad (15)$$

where  $\rho(A)$  is the spectral radius of  $A$  which is defined as the largest singular value of  $A$ . The terms  $X_\infty$  and  $Y_\infty$  are the solution to the controller and estimator Riccati equations given by:

$$X_\infty \equiv Ric(H_\infty) \geq 0 \quad , \quad Y_\infty \equiv Ric(J_\infty) \geq 0 \quad (16)$$

where  $H_\infty$  and  $J_\infty$  is given by following equation:

$$H_\infty \equiv \begin{bmatrix} A & \gamma^{-2} B_1 B_1^T - B_2 B_2^T \\ -C_1^T C_1 & -A^T \end{bmatrix} \quad (17)$$

$$J_\infty \equiv \begin{bmatrix} A^T & \gamma^{-2} C_1^T C_1 - C_2^T C_2 \\ -B_1 B_1^T & -A \end{bmatrix} \quad (18)$$

With considering  $A_\infty$  as follows:

$$A_\infty = A + \gamma^{-2} B_1 B_1^T X_\infty + B_2 F_\infty + Z_\infty L_\infty C_2 \quad (19)$$

Finally the  $H_\infty$  controller is given by:

$$K(s) \equiv \begin{bmatrix} A_\infty & -Z_\infty L_\infty \\ F_\infty & 0 \end{bmatrix} \quad (20)$$

The controller has the block structure as depicted in Fig. 1. This diagram presents that the controller consists of a dynamic observer which computes a state vector  $\hat{x}$  on the basis of measurements  $y$  and the control input  $u$ , and a feedback  $F$  maps  $\hat{x}$  to the control input  $u$ .

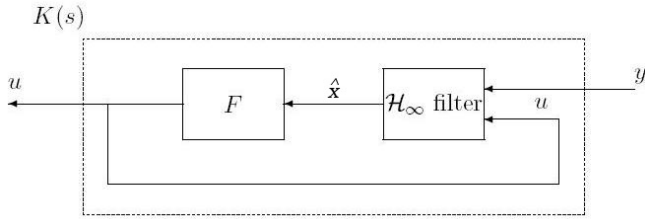


Fig. 1 Separation structure for the  $H_\infty$  controllers

### 3. $H_2$ /LQG Control Problem

The  $H_2$  optimal controllers coincide with the well known LQG controllers. The  $H_2$  optimal control problem is formalized as follows:

With considering eq.3, synthesize a stabilizing controller  $K$  for the generalized plant  $G$  such that  $\|T(s)\|_2$  is minimal. The solution of this important problem is split into two independent problems and makes use of a separation structure:

First, obtain an optimal state  $\hat{x}$  (state vector estimated by the Kalman filter) of the state variable  $x$ , based on the measurements  $y$ . Second, use this estimate  $\hat{x}$  as if the controller would have perfect knowledge of the full state  $x$  of the system. As is well known, the Kalman filter is the optimal solution to the first problem and the state feedback linear quadratic regulator is the solution to the second problem.

For the statement of  $H_2$ /LQG problem, a LTI system can be expressed by eq.5 to eq.8, that has a performance index (the cost function  $J_{LQG}$ ) as follows:

$$J_{LQG} = E \left\{ \int_0^\infty [x^T(t) u^T(t)] \begin{bmatrix} C_1^T \\ D_{12}^T \end{bmatrix} \begin{bmatrix} C_1 & D_{12} \end{bmatrix} \begin{bmatrix} x(t) \\ u(t) \end{bmatrix} dt \right\} \quad (21)$$

The  $H_2$ /LQG control problem computes a stabilizing

$H_2$  optimal LTI controller  $K$  for a partitioned LTI plant  $P$ .

As it was mentioned before, the first problem is solved by using a Kalman filter. This filter is a causal, linear mapping taking the control input  $u$ , and the measurements  $y$  as its inputs, and producing an estimate  $\hat{x}$  of the state  $x$  in such a way that the  $H_2$  norm of the transfer function from the noise  $w$  to the estimation error  $e = x - \hat{x}$  is minimal. The Kalman filter block diagram is shown in Fig. 2.

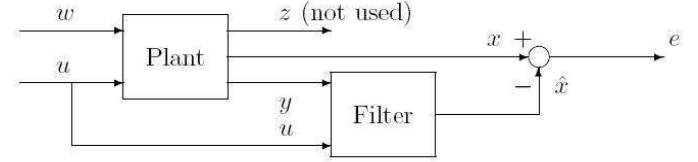


Fig. 2 The Kalman filter configuration

In this case, the optimal filter is given by the state space equation as follows:

$$\dot{\hat{x}} = A\hat{x} + B_2 u + K_{FC}(y - C_2 \hat{x} - D_{22} u) \quad (22)$$

In above equation, a Kalman filter with residual gain matrix  $K_{FC}$  is given by:

$$K_{FC} = (Y C_2^T + B_1 D_{21}^T)(D_{21} D_{21}^T)^{-1} \quad (23)$$

For the solution of the second problem, we consider the control law as follows:

$$f_{opt} = u = K_{FI} \hat{x} \quad (24)$$

where full-state feedback matrix  $K_{FI}$  is represented as follows:

$$K_{FI} = (D_{12} D_{12}^T)^{-1} (B_2^T X + D_{12}^T C_1) \quad (25)$$

Finally the  $H_2$ /LQG controller is given by:

$$k(s) = \begin{bmatrix} A - K_{FC} C_2 - B_2 K_{FI} + K_{FC} D_{22} K_{FI} & K_{FC} \\ -K_{FI} & 0 \end{bmatrix} \quad (26)$$

### 4. Modulation and Statement of Problem

#### 4.1. The model of study

Dynamic specifications of equipment such as stiffness or damping may influence decision making in case of modulation and designing methods. However, any semi-active control device should be in combination with base isolators to provide flexibility for lateral movement of equipment (See Fig. 3). Accordingly, Almazan et al. [1] compared the parameters of rigid and flexible structure (period of 0.5 second) on the FPS isolator. Results of such a comparison demonstrated that the difference between the drift of the isolator for both of these superstructures is very low. Although most of the equipment parts are rigid, even if they become flexible they will not have considerable effect on the response of the isolation system. Therefore,

in isolated equipment, response of the seismic isolator system is acquired with acceptable precision with the assumption of 'equipment+ raised floor' in the form of rigid mass. On the other side, based on the studies of Kulkarni and Jangid on a variety of isolators, we may modulate a superstructure for inconsiderably flexible

structures (such as multistorey buildings) in which the condition, response of the displacement of the isolator, and acceleration of the superstructure corresponds to the response of the actual model with higher precision [29].

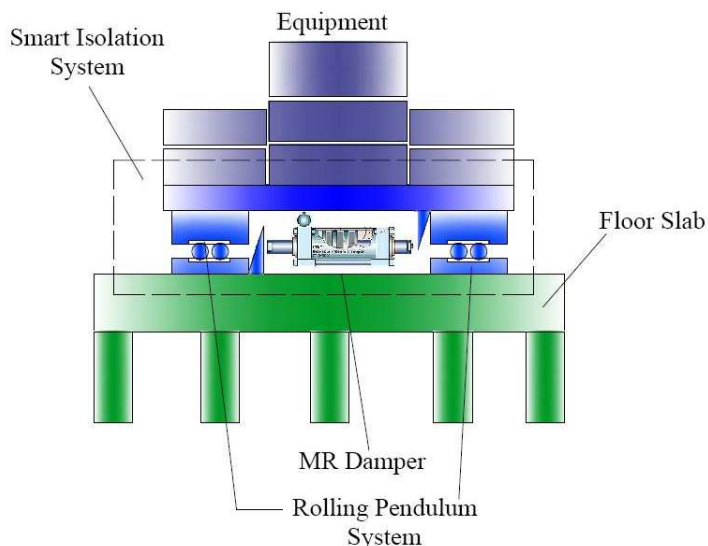


Fig. 3 Schematic model of a smart isolation system with MR damper

In this study, the 'equipment+ raised floor' model presented by Lambrou and Constantinou (1994) over computer centers has been used. Equipments, which are modulated in the form of one-degree of freedom over the raised floor, hold the main frequency of 40 Hz, and this corresponds to the former issues indicating use of rigid model for equipment. Fig. 3 represents the smart equipment isolation system using an MR damper and is considered in this study for seismic protection of equipment. To evaluate the potential of MR damper in structural control applications and to take full advantage of the unique features of this device, a model must be considered that can accurately reproduce the behavior of the MR damper. An MR damper together with a rolling pendulum system is installed between the equipment and the floor to reduce the vibration of the equipment. Based on the study by Yoshioka *et.al* (2002), the characteristics of the MR damper used in this study like maximum stroke, maximum force, and electric current are assumed as 3.5 cm, 50 N and 1.8A respectively.

#### 4.2. Mathematical model for analysis

Fig. 4 demonstrates a model with two-degrees of freedom which has been assumed for the control plan. Behavior of equipment and isolated raised floor are both assumed to be linear. The motion equations in the state space for the seismic isolator system are presented below;

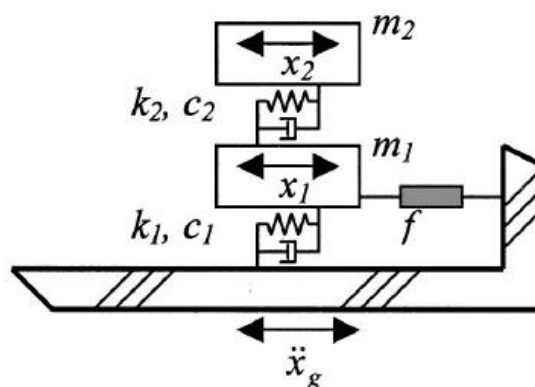
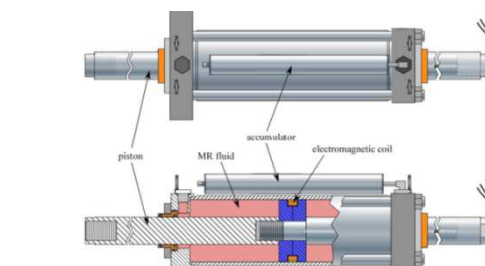


Fig. 4 Mathematical model for analysis

$$\dot{X} = AX + BU + E\ddot{x}_g \quad (27)$$

$$X = [x_1 \ x_2 \ \dot{x}_1 \ \dot{x}_2]^T \quad (28)$$

In this model,  $x_1$  and  $x_2$  are respectively the displacement of the raised floor and the equipment in comparison to the floor,  $u$  and  $\ddot{x}_g$  are the damper practiced control force and seismic acceleration of the storey.  $m_1$ ,  $m_2$ ,  $k_1$ ,  $k_2$ , and  $c_1$ ,  $c_2$  are respectively mass, damping, and stiffness coefficients for the raised floor and equipment. The other parameters in equation 27 are defined in the following equations;

$$A = \begin{pmatrix} [0] & [I] \\ -M^{-1}K & -M^{-1}C \end{pmatrix} \quad B = [0 \ 0 \ 1/m_1 \ 0]^T \quad (29)$$

$$E = [0 \ 0 \ -1 \ -1]^T$$

$$M = \begin{pmatrix} m_1 & 0 \\ 0 & m_2 \end{pmatrix} \quad K = \begin{pmatrix} k_1 + k_2 & -k_2 \\ -k_2 & k_2 \end{pmatrix} \quad (30)$$

$$C = \begin{pmatrix} c_1 + c_2 & -c_2 \\ -c_2 & c_2 \end{pmatrix}$$

Several mathematical models have been proposed for controllable fluid dampers. Spencer et al. [30] developed an effective model using the Bouc-Wen hysteresis model for MR fluid dampers. Because of the simple configuration of the MR damper used in this study, the damper dynamics can be represented with a combination of the Bouc-Wen model and a viscous damping element as shown in Fig. 5. This model is a special case of the model proposed by Spencer et al. (1997).

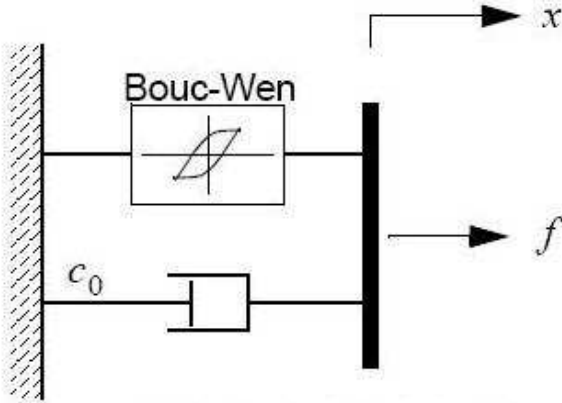


**Fig. 5** Magnetorheological damper model with Bouc-Wen hysteresis

The force generated by the MR damper shall be modeled as follows (Spencer et al. 2002):

$$F = c_0 \dot{x} + \alpha z \quad (31)$$

$$\dot{z} = -\gamma |\dot{x}| |z|^{n-1} - \beta \dot{x} |z|^n + A \dot{x} \quad (32)$$

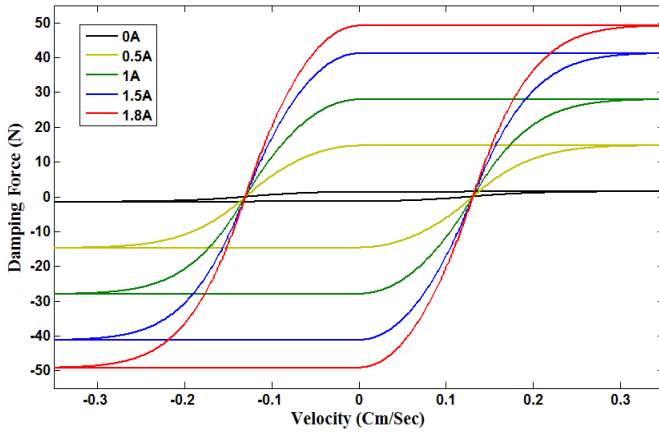
Based on the study by Yoshioka *et.al* [30], the parameters of the MR damper model is considered as  $\gamma = 1$ ,  $n = 1$ ,  $\gamma = \beta = 58.622 \text{ cm}^{-2}$  and  $c_0 = 0.3327 \text{ Ns/cm}$ . A small time lag exists between the command and the

damper force due to the inductance in the coil in the damper's electromagnet and the time constant of the fluid. This lag is modeled with a first-order filter between the control voltage  $v$  and the parameter  $\alpha(\frac{N}{\text{cm}})$  representing the damper yield level given by:

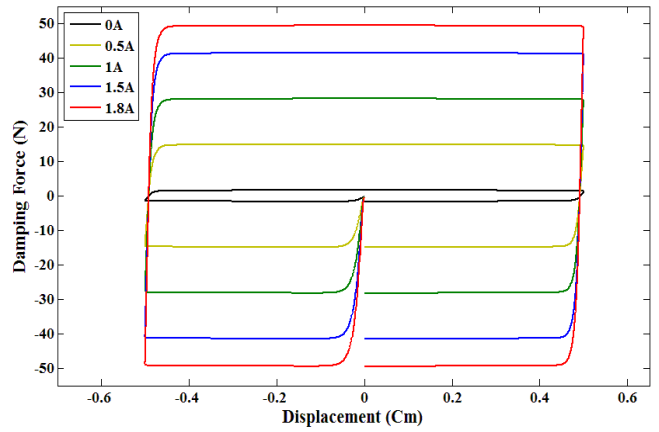
$$\dot{\alpha}(t) = -[\alpha(t) - p_1 v(t) - p_2] \eta \quad (33)$$

where,  $\eta = 2\pi \times 11.0(\frac{\text{rad}}{\text{s}})$ ;  $p_1 = 3111.7(\frac{\text{N}}{\text{cm}} \cdot \frac{\text{V}}{\text{V}})$ ; and  $p_2 = 161.47(\frac{\text{N}}{\text{cm}})$ .

In order to have an accurate verification, the responses of the MR damper at 1Hz sinusoid with an amplitude 15mm excitation for five constant electric current levels (Fig. 6) are compared to the results of the study by Spencer & Dyke[13] (Fig.7). Based on their studies, the response of the MR damper is considered for four constant voltage levels, 0V, 0.75V, 1.5V, and 2.25V. These voltages correspond to 0A, 0.25A, 0.5A, and 0.75A respectively. The force-velocity and the force-displacement loops in the both figure show that with the increase of the electric current, the damper force will markedly increase. It is also noted that in the force-velocity loop, due to the presence of an accumulation in the MR damper, the damper force is not exactly centered at zero velocity. According to these figures, the effects of changing the magnetic field are readily observed. At 0A the MR damper primarily exhibits the characteristics of a viscous device (i.e., the force-displacement relationship is approximately elliptical, and the force-velocity relationship is nearly linear).



(a)



(b)

**Fig. 6** Characteristics of an MR damper: (a) Force-velocity; (b) Force-displacement



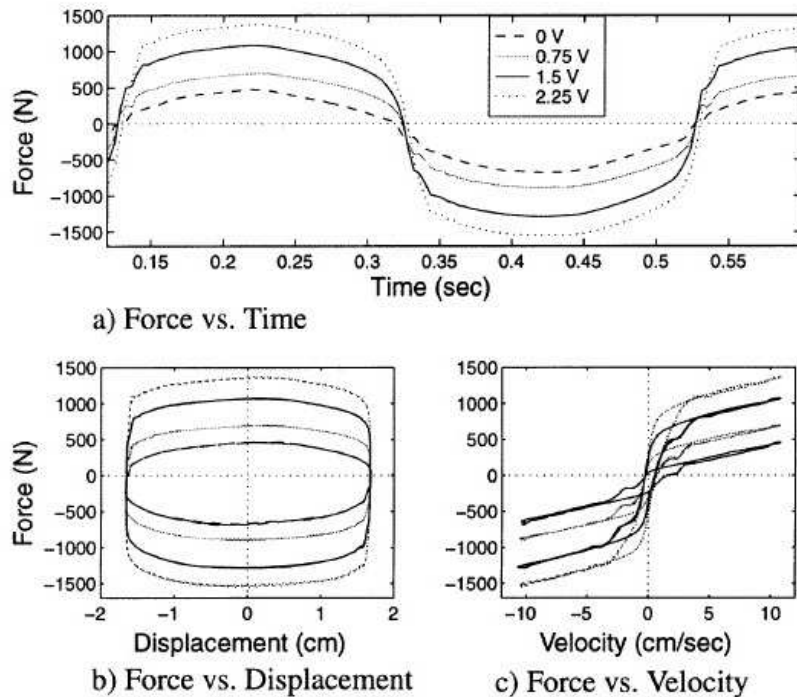


**Fig. 7** Characteristics of an MR damper: Force-velocity, and Force-displacement based on the study by Spencer & Dyke

MR dampers are nonlinear semi-active control devices that have significant potential to mitigate vibration and shocks. Because of their mechanical simplicity, high range and low power requirements, low cost, large force capacity, and robustness, these devices are suitable for various applications. Although they can only remove the energy from the system, recent studies have shown that the MR dampers can achieve the majority of the performance of fully active systems. (Jimenez et al. 2002; Gavin et al. 2005). Since smart damping devices such as MR dampers have highly nonlinear characteristics, a number of different control strategies have been proposed. Dyke and Spencer (1997) compared several control algorithms appropriate for a MR damper and concluded that a

clipped-optimal controller is most suitable for this class of dampers. The clipped-optimal controller employs a desired optimal control force that is determined using linear optimal control design strategies such as  $H_\infty$  and  $H_2/LQG$ , and then subsequently clips the force to accommodate the intrinsic dissipative nature of smart damping devices.

For this study, a clipped-optimal controller employing  $H_\infty$  and  $H_2/LQG$  strategies is used to reduce responses of the equipment. Spencer et al. (2000) and Ramallo et al. (2000a,b) showed through simulation that this approach is effective for smart semi-active systems. The basic concept of this methodology is shown in Fig. 8.

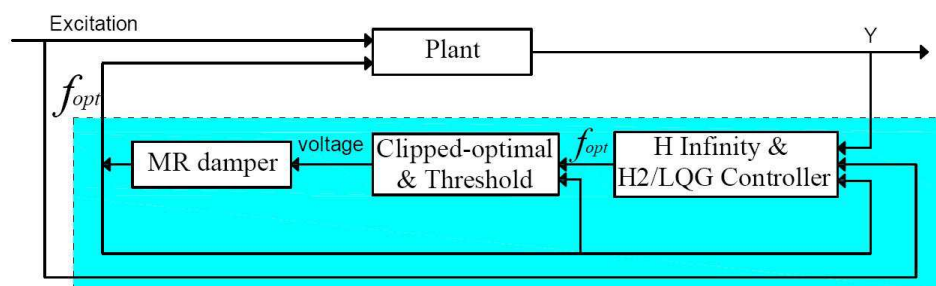


**Fig. 8** Semi-active algorithms with clipped-optimal switching

To track the optimal force that is obtained from Eqn.10 and Eqn.24 for  $H_\infty$  and  $H_2/LQG$  respectively, Dyke et al. (1996) proposed a clipped-optimal switching defined by:

$$v = V_{\max} H\{(f_{\text{opt}} - f_{\text{meas}})f_{\text{meas}}\} \quad (34)$$

where  $V_{\max}$  is voltage to the current driver associated with saturation of the magnetic field in the MR damper, and  $H(\bullet)$  is the Heaviside step function. This control algorithm has the benefit that a model of the damper is not required in the control design. In this study, an alternative clipped-optimal control (on-off type) with a threshold is proposed in which the control voltage remains zero below

minimum force,  $f_{min}$ . Thus voltage shall be obtained as follows:

$$v = \{V_{max} \cdot H\{(f_{opt} - f_{meas})f_{meas}\}, \quad (35)$$

$$v = 0 \quad \text{otherwise} \quad (36)$$

The force generated by the MR damper with and without clipped-optimal control under El Centro ground motion is shown in Fig. 9. As it is seen in this figure, the desired control forces which were created by two controllers ( $H_\infty$  and  $H_2/LQG$ ) and the generated clipped-optimal force by damper have been presented together. Their difference indicates to the distinctness of required force in ideal active control strategy with semi active control. Further, the command signal which is shown to

present state of being on/off and its value is schematic in the figures. The control force of damper is limited to saturation for 100 N. It is also quite remarkable that in the clipped-optimal control, if the generated force by the damper is in the same direction of the desired optimal force, the voltage applied to the current driver is increased to its maximum level.

The results of the studies by Spencer and Ramallo and Dyke and Spencer have been used for verification of the numerical model (Fig.10 & Fig.11) [13, 19 &22]. Fig. 11 may not be relevant to this study, as it is for different model and damper capacity; however there is type of similarity between their results in force and signal variation.

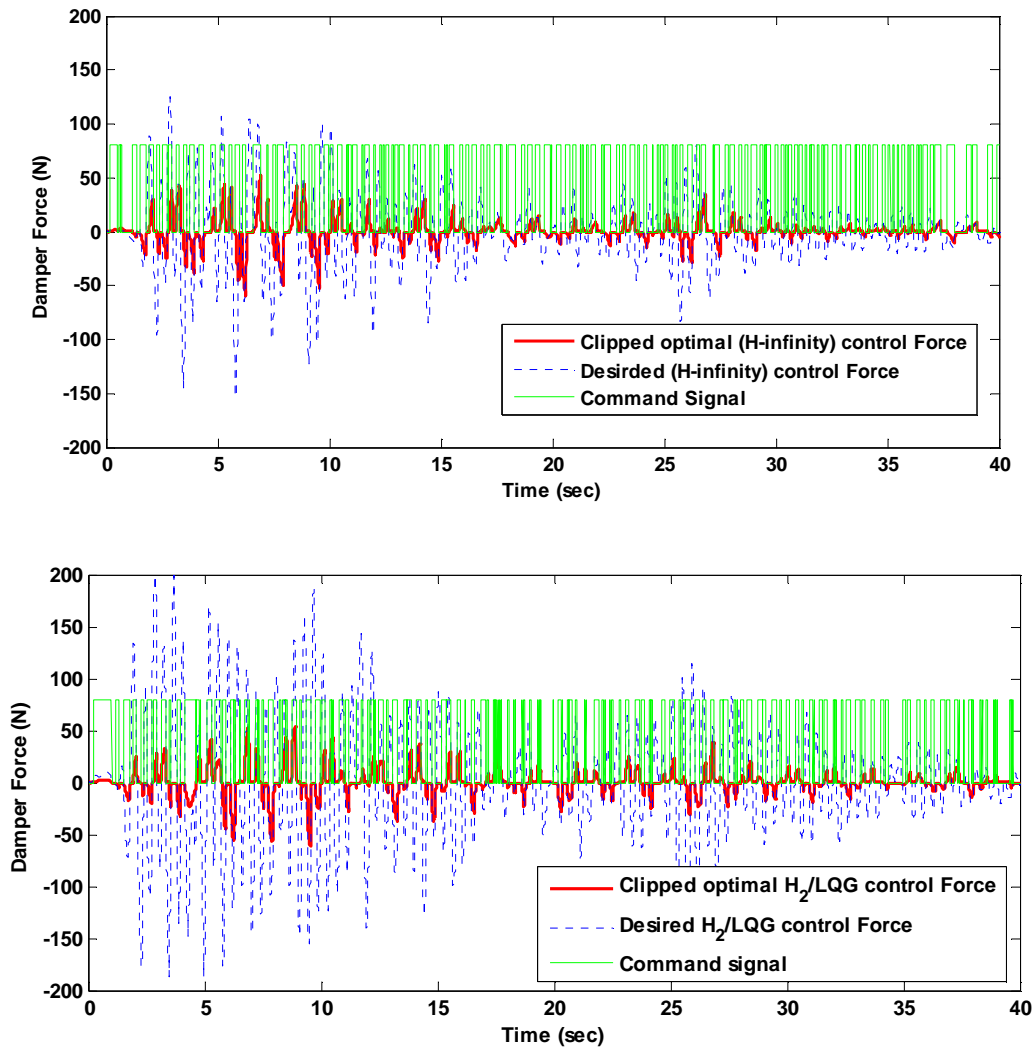


**Fig. 9** MR damper force and signal under El Centro ground motion, (a) clipped optimal and desire force for H-infinity controller, (b) clipped optimal and desire force for H2/LQG controller



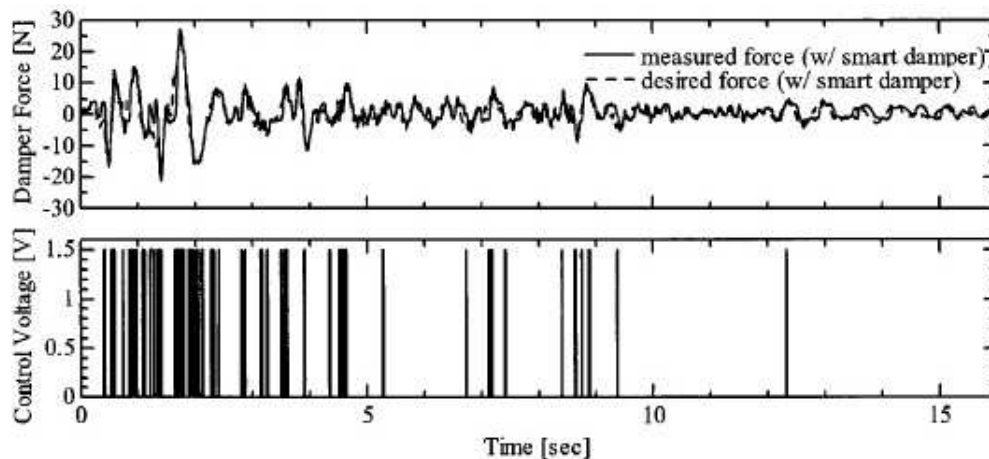


**Fig. 10** Experimental results due to El Centro based on the study by Spencer & Ramallo

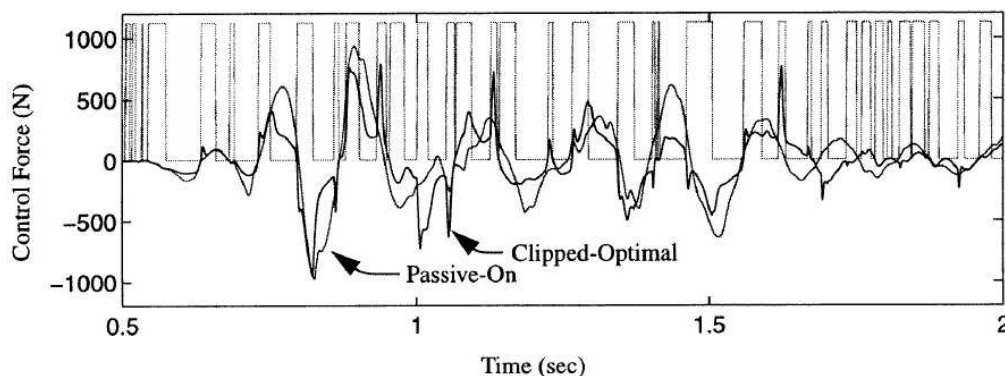


**Fig. 11** Command signal and control force applied in the clipped-optimal case and reaction force for the passive-on case due to El Centro based on the study by Spencer & Dyke

Force applied on the equipment inside of the building depends on the input seismic wave and structural specifications inside it. Therefore, in this study, the structural model used by Hamidi and ElNaggar which is a seven storey building is considered[20]. The 'equipment+ raised floor' model is mounted on the 4<sup>th</sup> and 7<sup>th</sup> floor of a seven storey building, which is a simplified model of a prototype seven storey R/C test structure used by the Japanese Building Research Institute (BRI) for some seismic research experiments [21]. Fig. 12 shows the floor-isolation system with the rolling pendulum system and semi-active controlled MR damper and represents a seven-storey building and raised floor, including mass, stiffness, and damping matrices. The masses of this structure are the same as those for the prototype seven

storey R/C building that was used by BRI for seismic researches [21]. The storey stiffness is selected so that the period of the first and second modes of the model is almost the same as those for the prototype building. Furthermore, the damping ratios for the first and second modes are the same as those for the real structure. Table.1 demonstrates that the specification of the "equipment+ raised floor" model has been used in this study.

The records selected as examples of ground motion imposed on structures are El Centro (1940), Kobe (1995), Northridge (1994), and Tabas (1978). The ground motion response of the 4<sup>th</sup> and 7<sup>th</sup> storey is used as input motion to investigate the effect of story level on efficiency of a semi-active system in protecting equipment. Properties of these earthquakes are represented in Table 2.

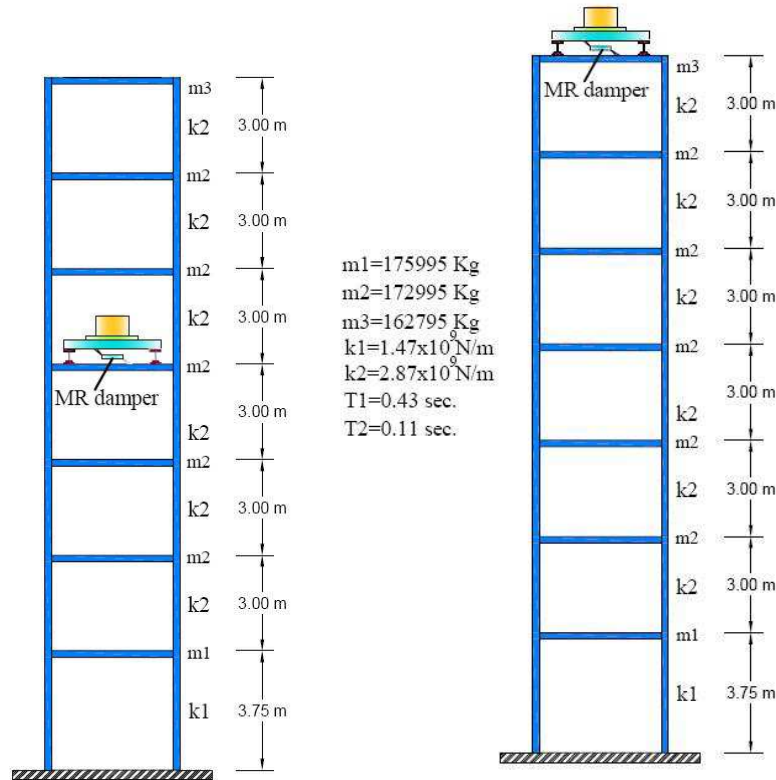


**Fig. 12** Shear building as the primary structure and a smart isolation system with an MR damper

**Table 1** Specification of “equipment+ raised floor” model

System	Specification	Values
Isolated Raised Floor	$m_1(\text{Kg})$	2631.53
	$k_1(\text{N/m})$	25946
	$c_1(\text{N.sec/m})$	330.5
	$\xi_1$	2%
	$T_1(\text{sec})$	2
	$m_2(\text{Kg})$	181.5
Equipment	$k_2(\text{N/m})$	11458874
	$c_2(\text{N.sec/m})$	1824
	$\xi_2$	2%
	$T_2(\text{sec})$	0.025

**Table 2** Specifications of the Input ground motions

Event	Year	Mw	PGA(g)	Station	R(km)	Mechanism
El Centro	1940	7	0.31	El Centro Array#9	8.3	Strike-slip
Kobe	1995	6.9	0.82	KJMA	0.6	Strike-slip
Northridge	1994	6.7	0.61	Beverly Hills-12520 Mulhol	20.8	Reverse-slip
Tabas	1978	7.4	0.84	Tabas	5.2	Strike-slip

## 5. Discussing on Results

Herein response of the equipment along with the seismic isolator with an MR damper settled over a raised floor was studied under four different ground motions recorded on the 4<sup>th</sup> and 7<sup>th</sup> stories. A natural period of two seconds for an isolated raised floor was assumed. Thus, by using an MR damper with two different algorithms and two measuring accelerations and displacement sensors laid

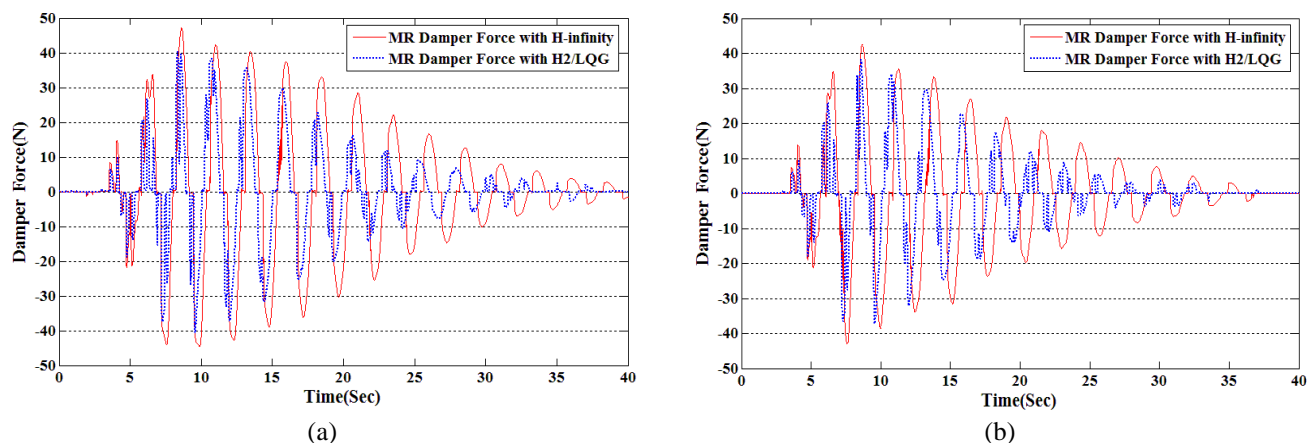
between the floor and equipment (beside of MR damper), the responses were compared with passive strategy.

### 5.1 Comparing obtained results with isolation systems

Fig. 13(a) and (b) illustrate the force generated by an MR damper in the 4<sup>th</sup> and 7<sup>th</sup> stories when the damper is controlled by two different clipped-optimal  $H_\infty$  and  $H_2$ /LQG algorithms under Northridge ground motion. As

shown, the generated force by employing the clipped-optimal with  $H_\infty$  algorithm is higher than controlling the system with  $H_2/LQG$  algorithm. As will be discussed later, higher damper force results in a lower level of maximum responses of the equipment. This conclusion is achieved

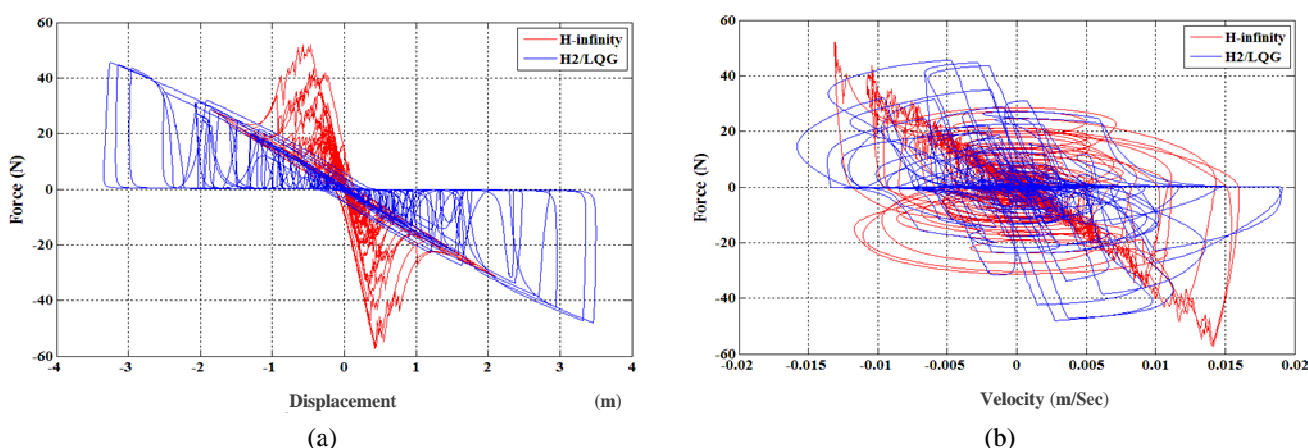
for three other different ground motions. Further analysis show on the 4<sup>th</sup> floor, due to lower input excitation induced, damper force is reduced and the application of the  $H_\infty$  algorithm has a lower efficiency in comparison with the  $H_2/LQG$  algorithm.



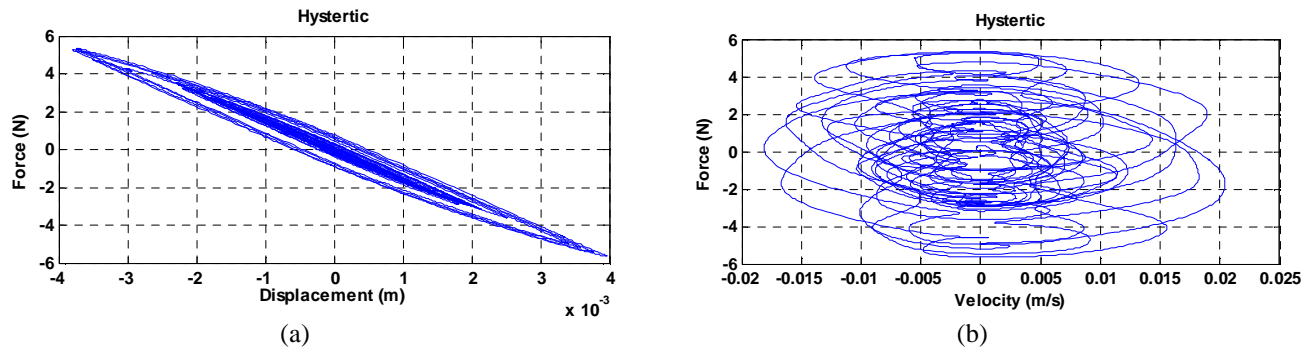
**Fig. 13** Comparison an MR damper force using  $H_\infty$  algorithm and  $H_2/LQG$  algorithm (Northridge ground motion) (a) in 7<sup>th</sup> storey, (b) in 4<sup>th</sup> storey

Fig.14 (a) and (b) show the comparison of hysteresis loops for both clipped-optimal  $H_\infty$  and  $H_2/LQG$  algorithms under El Centro ground motion. Comparing the command voltage time histories, both of the two semi-active control cases can generate the smooth and continuously varying command voltages. This leads to better acceleration reduction for the two semi-active control cases. It has to be mentioned that a smart semi-active system with an MR damper has rounded corners on the loops and gave moderate acceleration levels. Also as it is shown in Figure 14(a), the clipped-optimal  $H_\infty$  algorithm can generate

almost the same force but with considerable differences in displacement (the system can achieve better performance), and this matter indicates the efficiency of this algorithm in comparison with the  $H_2/LQG$  algorithm. Also this concept is observable in the case of the force-velocity loop. Fig. 15 presents variation of force-displacement and force-velocity in passive system under El Centro ground motion. As seen in this figure, the required controlling force in passive systems is about 0.1 time of the semi active system.



**Fig. 14** Comparison (a) force-displacement and (b) force-velocity of smart system with an MR damper using  $H_\infty$  algorithm and  $H_2/LQG$  (El Centro ground motion)

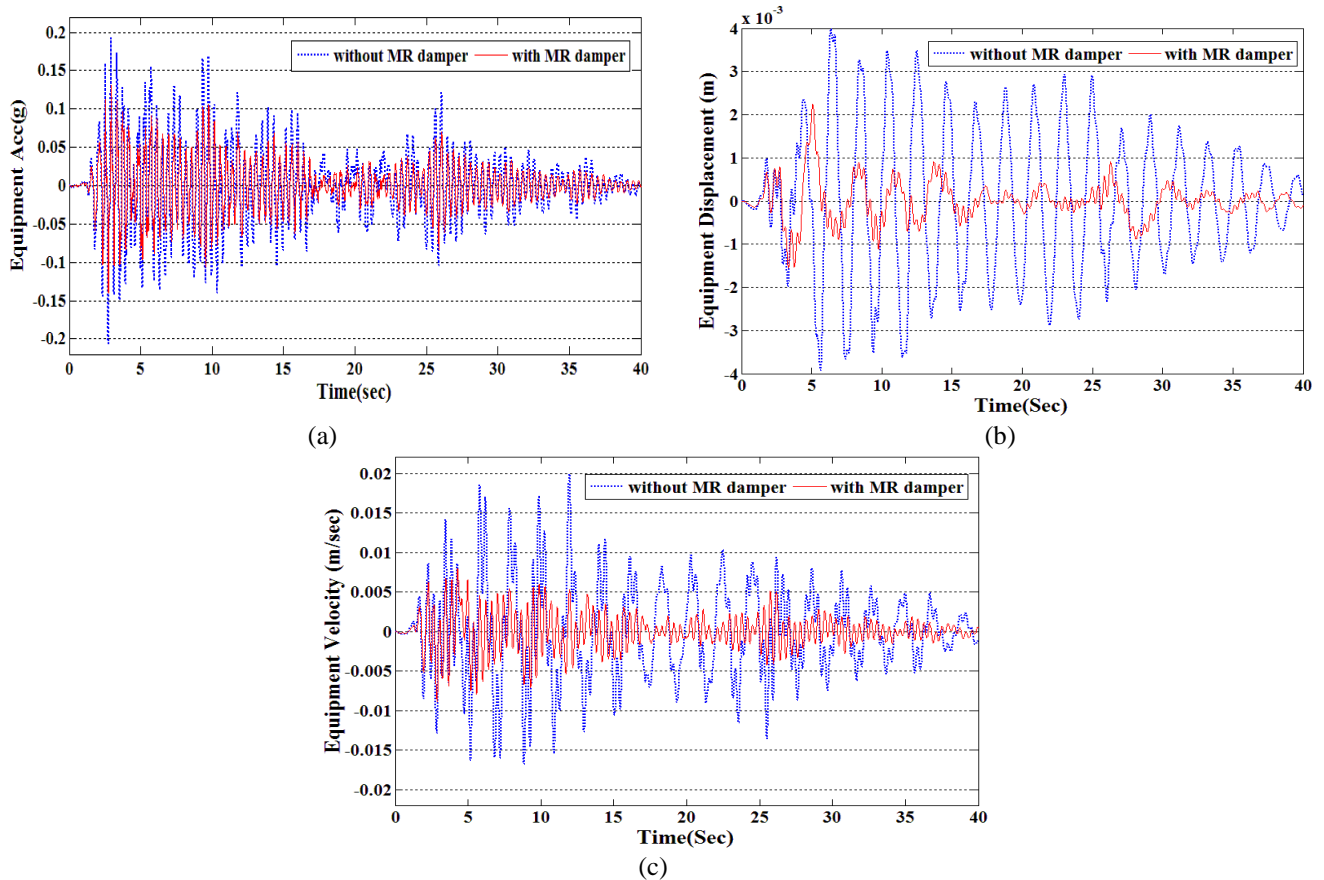


**Fig. 15** Comparison (a) force- displacement and (b) force-velocity of passive damper (El Centro ground motion)

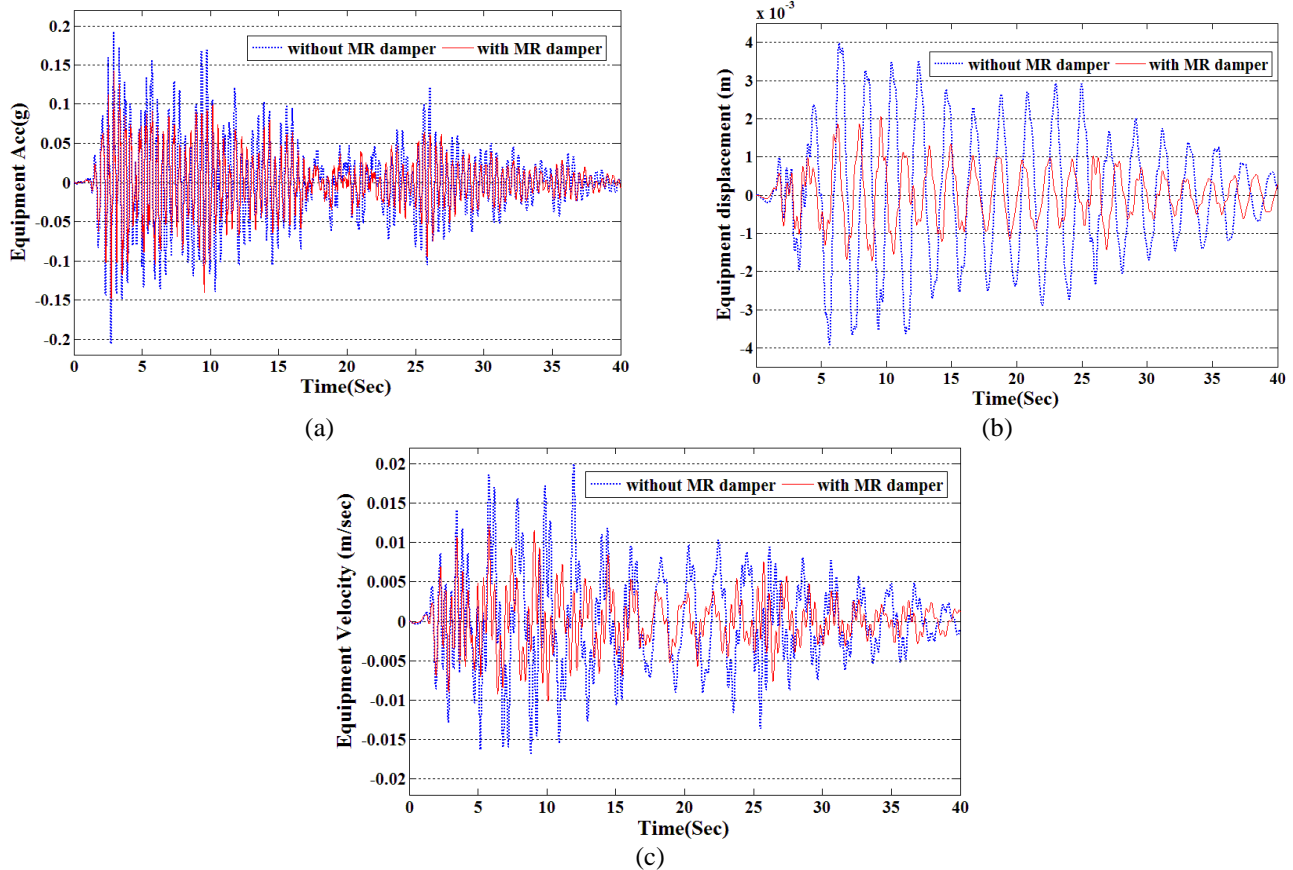
In Fig. 16, time history acceleration, relative displacement, and velocity response of equipments with an MR damper are compared with seismic isolated equipment (without an MR damper). In this figure, the responses of equipment under El Centro ground motion on the 7<sup>th</sup> storey are illustrated when the MR damper is controlled with the clipped-optimal  $H_\infty$  algorithm. Comparison of the results shows the maximum acceleration and displacement of equipments are reduced 40% and 70% respectively by using an MR damper. These results express the fully effective performance of a smart semi-active system under the  $H_\infty$  control algorithm. Furthermore, the reduction rate is up to 75% in the relative velocity of the system in times

around 11-14 seconds.

Fig. 17 represents the same comparison between responses of the equipment with and without an MR damper when the semi-active control algorithm is a clipped-optimal using  $H_2$ /LQG. In this condition, maximum acceleration under the El Centro earthquake using an MR damper is reduced around 30% while maximum displacement and relative velocity reduction rate is up to 50%. These results support the higher efficiency of a semi active control with clipped-optimal  $H_\infty$  algorithm in comparison with  $H_2$ /LQG algorithm as well.



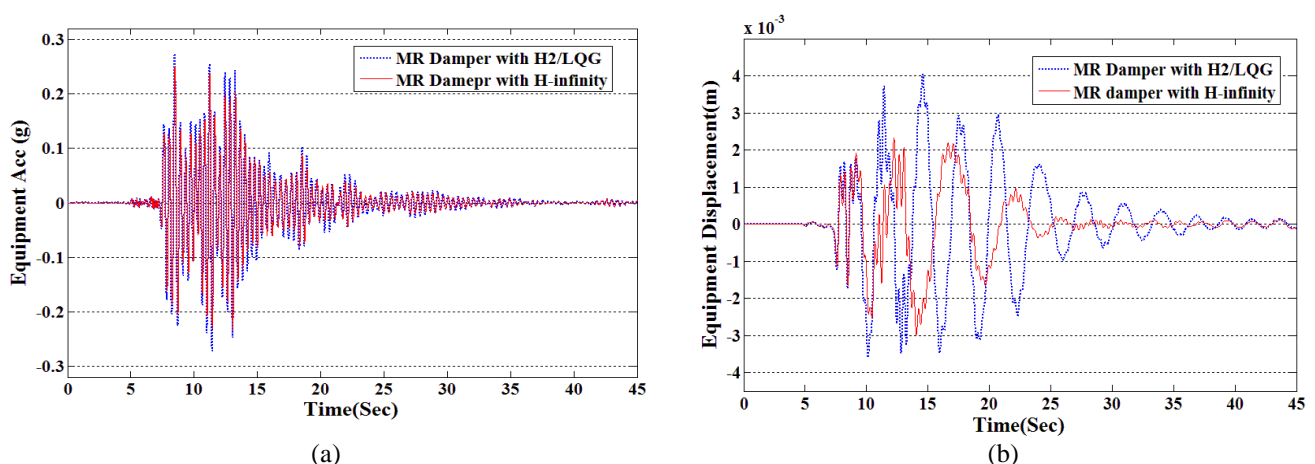
**Fig. 16** Comparison (a) acceleration, (b) relative displacement and (c) relative velocity response of equipments with an MR damper using  $H_\infty$  algorithm and seismic isolation system (El Centro ground motion)



**Fig. 17** Comparison (a) acceleration, (b) relative displacement and (c) relative velocity response of equipments with an MR damper using  $H_2/LQG$  algorithm and seismic isolation system (El Centro ground motion)

In order to have direct evaluation regarding the control algorithms, seismic response time histories of the equipment settled over an MR damper with both algorithms is illustrated in Fig. 18. In this figure, two different responses of equipment on the 7<sup>th</sup> storey are compared under Kobe ground motion. As it is shown,

maximum acceleration in the case of  $H_2/LQG$  is about 0.28g in time 12 seconds whereas this value in the same time for  $H_\infty$  is about 0.24g. Also it is obvious that the  $H_\infty$  algorithm has declined the response of displacement effectively in comparison with the  $H_2/LQG$  algorithm.



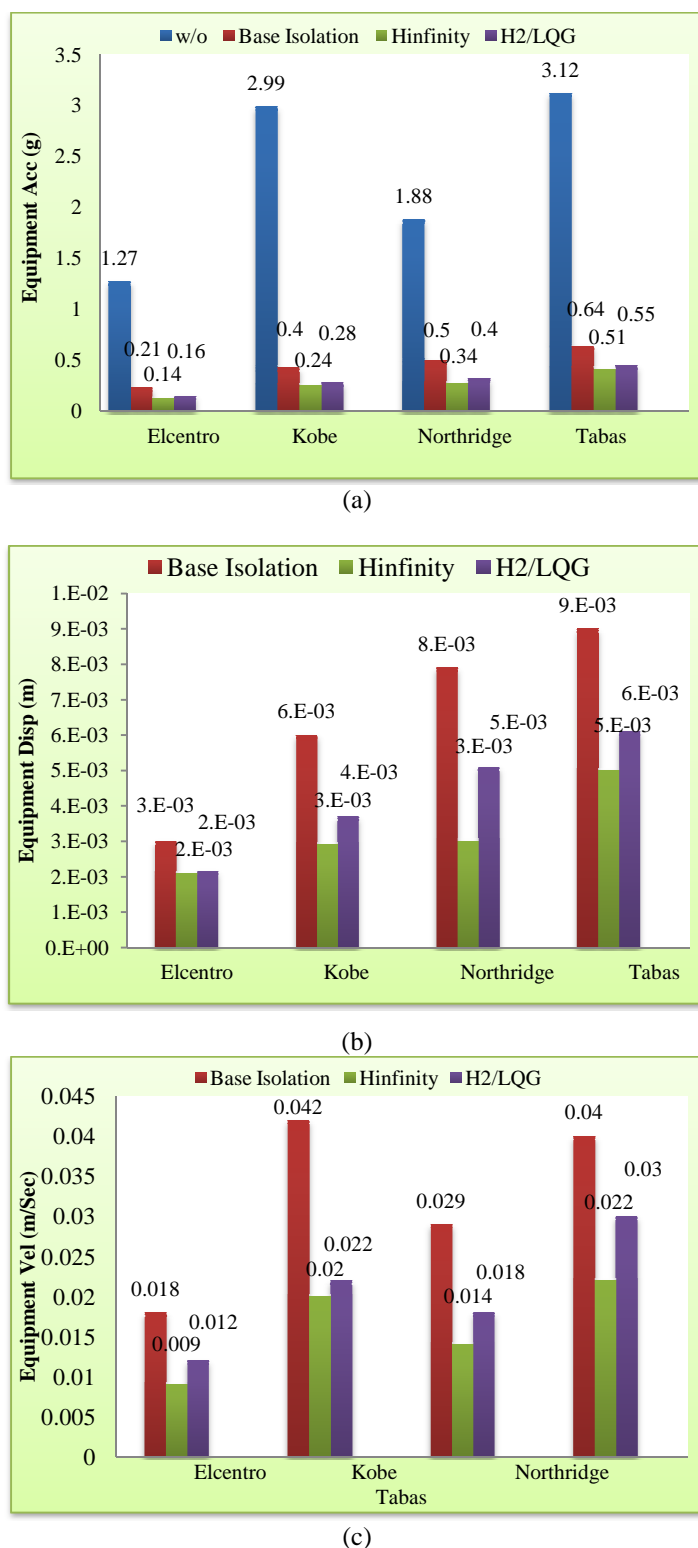
**Fig. 18** Comparison (a) acceleration, (b) relative displacement response of equipments with an MR damper using  $H_\infty$  algorithm and  $H_2/LQG$  algorithm (Kobe ground motion) in 7<sup>th</sup> floor

Fig. 19 (a), (b) and (c) compare the response of acceleration, displacement, and velocity of the system making use of an MR damper and seismic isolator for the sake of 7<sup>th</sup> floor and under entire 4 seismic types

respectively. The general point in the case of the performance of the system is that for the El Centro, Kobe and Northridge earthquakes, performance of the system is very effective in the reduction of the maximum

acceleration, lateral displacement, and velocity. For all 4 quakes, performance of the smart system in reduction of equipment acceleration with  $H_\infty$  is better than with the  $H_2/LQG$  algorithm. In addition, this reduction is more obvious for Northridge. It has to be mentioned that MR damper with clipped-optimal control and  $H_\infty$  algorithm perform better in comparison to the latter algorithm,

specifically in the decrease of equipment displacement. This reduction is more observable in case of Kobe. These figures demonstrate that the system acquires great performance with both  $H_\infty$  and  $H_2/LQG$  algorithm in the reduction of equipment velocity.



**Fig. 19** Comparison: (a) maximum acceleration response; (b) maximum displacement response; (c) maximum velocity response of equipments under different control strategy in 7<sup>th</sup> floor



## 6. Conclusions

In this study, the protection of sensitive equipment inside buildings against seismic ground motion was investigated because these vulnerable components may be damaged and the consequence of their damages may be irrecoverable. Efficacy of semi-active devices such as an MR damper to seismic response of equipment was investigated with clipped-optimal control in combination with two robust algorithms,  $H_\infty$  and  $H_2/LQG$  in comparison with passive seismic isolation strategy. The investigation was carried out in a seven storey generic building and on two different levels (4<sup>th</sup> and 7<sup>th</sup> floors) of the structure.

The results acquired presented that the seismic isolator has considerably reduced the acceleration of the equipment but it has compensated by increasing the response of displacement and velocity. However, using an MR damper improved the response of the seismic isolator and reduced the lateral displacement of the isolator and the acceleration as well. Considering the acquired results, it was made clear that the function of the smart semi-active device (MR damper) with clipped-optimal control and  $H_\infty$  and  $H_2/LQG$  algorithms is effective in reducing the acceleration of all ground motions. Results also indicate that the function of the considered system is effective in reducing the response of displacement and velocity under all earthquake types. Finally, according to the carried out study, as expected, it was discovered that the MR damper with the  $H_\infty$  control algorithm (by considering the effect of external disturbances and excitations) has a better performance remarkably in the reducing response of acceleration, displacement, and velocity of the equipment for both stories in comparison with the  $H_2/LQ$  algorithm.

## References

- [1] Almazan JL, De La Llera JC, Inaudi JA. Modeling aspect of structural isolated with the frictional pendulum system, *Earthquake Engineering Structure*, 1998, Vol. 27, pp. 845-867.
- [2] Christenson RE. Semi-Active Control of Civil Structures for Natural Hazard Mitigation: Analytical and Experimental Studies, M.Sc. thesis, University of Notre Dam Indiana, 2001.
- [3] Chen G, Chen C. Semi-active control of a 20-storey benchmark building with piezoelectric friction dampers, *Journal of Engineering Mechanic*, 2004, Vol. 130, pp. 393-400.
- [4] Lambrou V, Constantinou. MC. Study of seismic isolation systems for computer floors, Technical Report, NCEER-94-0020, 1994.
- [5] Yang JN, Agrawal AK. Semi-active hybrid control systems for nonlinear building against near-fault earthquakes, *Engineering Structure*, 2002, Vol. 24, pp. 71-80.
- [6] Xu YL, Yang ZC, Chen J, Liu HJ, Chen J. Microvibration control platform for high technology facilities subject to traffic-induced ground motion, *Engineering Structures*, 2003, Vol. 25, pp. 1069-1082.
- [7] Xu YL, Li B. Hybrid platform for high-tech equipment protection against earthquake and microvibration, *Earthquake Engineering & Structural Dynamics*, 2006, No. 8, Vol. 35, pp. 943-967.
- [8] Christenson RE, Spencer BF, Johnson EA, Seto K. Coupled building control using smart damping strategies, *Proceeding of SPIE Smart Structures and NDE Symposia*, 2000, 9 p.
- [9] Sahasrabudhe S, Nagarajaiah S. Semi-active control of sliding isolated bridges using MR dampers, *Earthquake Engineering and Structural Dynamics*, 2005, Vol. 34, pp. 965-983.
- [10] Francis BA. A Course in  $H_\infty$  Theory, Springer, Berlin, 1987.
- [11] Symans MD, Constantinou MC. Seismic testing of a building structure with a semi-active fluid damper control system, *Earthquake Engineering and Structural Dynamics*, 1997, Vol. 26, pp. 759-770.
- [12] Dyke SJ. Acceleration Feedback Control Strategies for Active and Semi-Active Control Systems: Modeling, Algorithm Development, and Experimental Verification, P.H.D Dissertation, University of North Dame, Indiana, 1996.
- [13] Dyke SJ, Spencer BF, Sain MK, Carlson JD. An experimental study of MR dampers for seismic protection, *Smart Materials and Structures*, 1998, Vol. 7, pp. 693-703.
- [14] Dyke SJ, Spencer BF, Sain MK, Carlson JD, Modeling and control of magnetorheological dampers for seismic response reduction, *Smart Materials and Structures*, 1996, Vol. 5, pp. 565-575.
- [15] Shook D, Lin P, Lin T, Roschke PN. A comparative study in the semi-active control of isolated structures, *Smart Materials and Structures*, 2007, No. 4, Vol. 16, doi:10.1088/0964-1726/16/4/058.
- [16] Lin P, Loh C. Semi-Active Control of Floor Isolation System Using MR-Damper, Sensors and Smart Structures Technologies for Civil, Mechanical, and Aerospace Systems, *Proceedings of SPIE 6932*, 2008, Vol. 69320U.
- [17] Liu M. Robust  $H_\infty$  control for uncertain delayed nonlinear systems based on standard neural network models, *Neurocomputing*, 2008, Vol. 71, pp. 3469-3492.
- [18] Lin PY, Roschke PN, Loh CH. Hybrid base-isolation with magnetorheological dampers and fuzzy control, *Structural Control and Health Monitoring*, 2007, Vol. 3, pp. 384-405.
- [19] Fan Y. Ch, Yang JN, Lin PY. Experimental performance evaluation of an equipment isolation using MR dampers, *Earthquake Engineering and Structural Dynamics*, 2009, Vol. 38, pp. 285-305.
- [20] Lyan YL, Ging LL. Predictive control of smart isolation system for precision equipment subject to near-fault earthquakes, *Journal of Engineering Structures*, 2007, Vol. 43, pp. 1-20.
- [21] Ramallo JC, Johnson EA, Spencer BF Jr. Smart base isolation systems, 14th Analysis and Computational Specialty Conf. Proc, Structures Congress & Exposition, Philadelphia, 2000.
- [22] Hamidi M, El Naggar. On the performance of SCF in seismic isolation of the interior equipment of buildings, *Earthquake Engineering and Structural Dynamics*, 2007, Vol. 36, pp. 1581-1604.
- [23] Okamoto S, Nakata S, Kitagawa Y, Yoshimura M. A progress report on the full-scale seismic experiment of a seven story reinforced concrete building – part of the US-Japan cooperative program, Research paper No 94, Building Research Institute, 1989.

- [24] Spencer BF Jr, Johnson EA, Ramallo JC. Smart isolation for seismic control, JSME International Journal Series C: Special Issue on Frontiers of Motion and Vibration Control, 2000, No. 3, Vol. 43, pp. 704-711.
- [25] Narasimhan S, Nagarajaiah S. Smart base isolated benchmark building part II: Phase I sample controllers for linear isolation system, Journal of Structural Control, 2002, Vol. 1, pp. 1-17.
- [26] Yang JN, Lin S, Jabbari F.  $H_2$ -based control for civil engineering structures, Structural Control and Health Monitoring, 2003, Vol. 10, pp. 205-230.
- [27] Yang JN, Lin S, Jabbari F.  $H_\infty$ -based control for civil engineering structures, Structural Control and Health Monitoring, 2004, Vol. 11, pp. 223-237.
- [28] Narasimhan S, Nagarajaiah S. Smart base isolated buildings with variable friction systems:  $H_\infty$  controller and SAIVF device, Earthquake Engineering and Structural Dynamics, 2006, Vol. 35, pp. 921-942.
- [29] Nagarajaiah S, Narasimhan S. Seismic control of smart base isolated buildings with new semi-active variable damper, Earthquake Engineering and Structural Dynamics, 2007, Vol. 36, pp. 729-749.
- [30] MATLAB, The Math Works, Inc, Natick, MA, 2000.
- [31] Ramallo JC, Johnson EA, Spencer BF Jr, Sain MK. Smart base isolation systems, Proceedings of the Advanced Technology in Structural Engineering, Structures Congress, Philadelphia, 2000a.
- [32] Kulkarni JA, Jangid RS. Rigid body response of base-isolated structures, Journal of Structural Control, 2001, Vol. 9, pp. 171-188.
- [33] Yoshioka H, Ramallo JC, Spencer BF. Smart base isolated strategies employing magnetorheological dampers, Engineering Mechanics, 2002, Vol. 128, pp. 540-551.